Relativistic Channeling of a Picosecond Laser Pulse in a Near-Critical Preformed Plasma

M. Borghesi, A. J. MacKinnon, L. Barringer, R. Gaillard, L. A. Gizzi,* C. Meyer, and O. Willi
Imperial College of Science, Technology and Medicine, London, United Kingdom

A. Pukhov† and J. Meyer-ter-Vehn
Max-Planck-Institut für Quantenoptik, D-85748 Garching, Germany
(Received 23 September 1996)

Relativistic self-channeling of a picosecond laser pulse in a preformed plasma near critical density has been observed both experimentally and in 3D particle-in-cell simulations. Optical probing measurements indicate the formation of a single pulsating propagation channel, typically of about 5 μm in diameter. The computational results reveal the importance in the channel formation of relativistic electrons traveling with the light pulse and of the corresponding self-generated magnetic field. [S0031-9007(97)02324-7]

PACS numbers: 52.40.Nk, 52.60.+h, 52.65.Rr, 52.70.Kz

The study of the interaction of intense laser pulses with plasmas is relevant for a number of applications, such as particle acceleration by plasma waves [1] and the fast ignitor scheme [2] for inertial confinement fusion. These applications require the pulse to propagate over several Rayleigh lengths without considerable energy loss. It has been shown that the propagation of high intensity pulses through initially neutral gases can be affected by ionization induced defocusing [3]. The use of preformed plasma channels [4] appears to be an effective way to overcome this limitation. For sufficiently powerful, spatially uniform laser pulses, self-guiding of the pulse due to relativistic effects is also possible [5]. Channeled propagation at relativistic intensities through initially neutral gases has been already observed in various experiments [6,7]. The propagation through preionized plasmas of near critical density, particularly relevant for fast ignitor applications, has been studied in the past using 100 ps pulses at irradiances below 10^{16} W/cm^2 [8]. An experimental study of propagation at relativistic intensities in such plasmas, also presenting experimental observations of relativistic channeling, is presently in print [9]. Recently, three-dimensional particle-in-cell (3D PIC) simulations have been reported for laser pulse propagation in near-critical underdense plasmas far above the threshold for relativistic filamentation [10]. The key feature predicted by these simulations is the formation of a narrow, single propagation channel, containing a significant part of the laser energy. The simulations reveal the importance of relativistic electrons traveling with the light pulse and generating multimegagauss magnetic fields that strongly influence light propagation.

This Letter presents experimental and computational evidence of a single channel formation in the case of a picosecond laser pulse propagating in a preformed, fully ionized near-critical plasma with a density gradient in the laser direction. Channeling of the pulse was observed in interferometric images and through intense, localized plasma emission. Spectrally resolved measurements of the backscattered radiation were consistent with channeling of the laser pulse. The experiment was modeled with a 3D PIC code, and very good agreement between the experimental results and the simulations was observed.

The experiment was performed at the Rutherford Appleton Laboratory using the Vulcan Nd:glass laser in the chirped pulse amplification (CPA) mode. The experimental arrangement is shown in Fig. 1. The targets were plastic (CH or Formvar) films with a thickness between 100 and 500 nm. The plasma was performed by a 400 ps pulse, frequency doubled in a KDP crystal to $\lambda = 0.527$ μm, which was focused onto target, in a spot between 200 and 300 μm in diameter, at an irradiance below 10^{13} W/cm^2. A 1.054 μm CPA interaction pulse 1 ps in duration was focused into the preformed plasma. Both the heating and the interaction pulse were focused onto target by the same $F/4.5$ off-axis parabola (OAP). The green heating beam was injected into the short pulse beam line through the back of the last turning mirror before the OAP. A small divergence was imposed on the heating beam before the interaction chamber by a telescope in order to obtain a larger focal spot. The focusability of

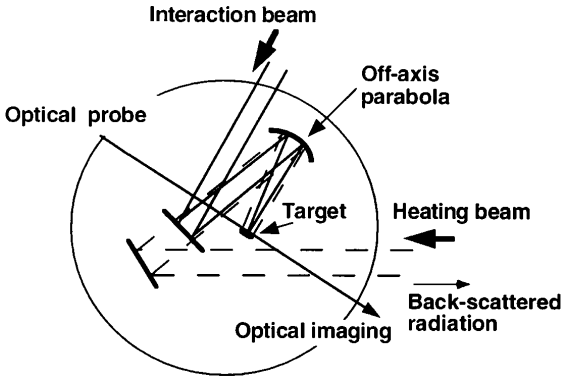

FIG. 1. Schematic of the experimental arrangement.

the CPA beam was investigated in a separate experiment, measuring the laser energy transmitted through pinholes of different diameters [11]. The beam was found to be about 3.5 times diffraction limited. This resulted, with the $F/4.5$ focusing optics, in a $12-15$ μm full width at half maximum (FWHM) focal spot. With an average interaction power of 10 TW, an incident irradiance between 5 and 9×10^{18} W/cm^2 was obtained. The delay between heating and interaction pulses was varied, allowing interaction with the plasma at different stages of its evolution.

The plasma was diagnosed with a temporally independent probe pulse which was split off from the uncompressed interaction beam. The probe beam was compressed by a pair of gratings and frequency doubled in a KDP crystal resulting in a probe wavelength of 0.527 μm and a pulse duration of a few picoseconds. The spatial resolution determined by the optical system was around $2-3$ μm. Time-resolved density maps of the preformed plasma were obtained with a Nomarski modified interferometer [12]. The preformed plasma density characterization was limited to electron densities lower than 1×10^{20}/cm^3, due to refraction of the probe beam off the steep density gradients present in the inner part of the plasma. Calculated results, obtained with the 1D hydrodynamic code MEDUSA [13], were used in the analysis for the plasma regions not accessible experimentally. Time-resolved Schlieren photography with a sensitivity of 5 mrad was used to image the density gradient distribution in the plasma. The light collected onto the detector was spectrally filtered around the probe wavelength, i.e., the second harmonic of the interaction pulse wavelength. Consequently, the time-integrated second harmonic emission from the plasma was also imaged onto the film, and was superimposed on the Schlieren pictures. Spectra of the backscattered radiation were collected with an optical grating spectrometer, using a 1200 lines/mm grating (linear dispersion 15 Å/mm).

Self-channeling of the CPA pulse appeared to be a typical feature of the interaction in the investigated experimental conditions and was detected via optical probe measurements. The Schlieren image of Fig. 2 refers to the interaction of a 10 TW pulse with the preformed plasma. The measured density profile is also shown (1D simulations predict that the plasma is fully ionized, with a peak density of about 5×10^{20}/cm^3). The most striking feature in the picture is the narrow optical emission filament clearly visible in the center of the plasma. The channel-like emission is time integrated and is due to second harmonic (2ω) light emitted during the interaction, produced via nonlinear processes in correspondence with the large density and intensity gradients present inside the channel [14]. It can therefore be interpreted as a signature of the spatial extent of the interaction beam in the plasma. In Fig. 2 the second harmonic emission is superimposed on the Schlieren image, which is time resolved and depicts the density gradient distribution in the plasma 30 ps after the interaction.

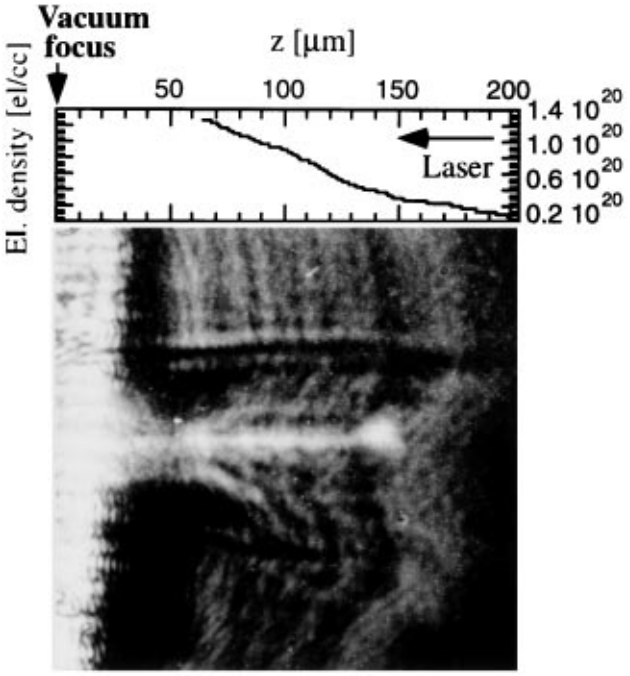

FIG. 2. Time-resolved Schlieren image taken 30 ps after the interaction of a 1 ps, 1.054 μm pulse at an irradiance between 5 and 9×10^{18} W/cm^2 with the preformed plasma. The narrow channel feature visible in the center of the plasma is time integrated and is due to second harmonic emitted during the interaction. The density profile of the preformed plasma along the laser axis is shown. z is the distance from the original target position.

The features of the channel structure are more clearly visible in Fig. 3, where the self-emission of Fig. 2 has been isolated. The diameter of the channel is about 5 μm and its length about 130 μm. Closer observation reveals that the channel changes in size periodically over distances of $15-20$ μm with the transverse dimension varying within a few microns. Similar features have been observed near the relativistic self-focusing threshold [6]. From comparison with the preformed plasma profile, it can be seen that the laser pulse focuses down to 5 μm in size at a density of around 0.05 times the critical density n_c ($n_c \sim 1 \times 10^{21}/$ cm^3 for $\lambda = 1$ μm). It should also be noted that the laser power was about 25 times the threshold power for relativistic self-focusing, $P_{\text{th}} = 17\omega^2/\omega_p^2 \approx 0.4$ TW at this density.

Evidence of channeling was also obtained from interferometric measurements. The interferogram of Fig. 4 was taken at about 5 ps after the interaction (the preformed plasma density profile is also shown). A front (due to the shock wave expanding in the preformed plasma) produced by the short pulse while focusing down into the channel is clearly visible. The laser pulse appears to be focused with an $F/4.5$ cone up to a background density of approximately 0.07 n_c at a distance of

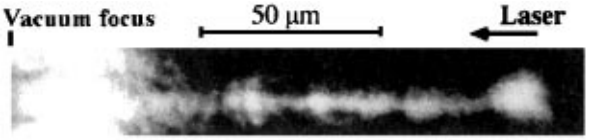

FIG. 3. Self-emission ($\lambda = 0.527\ \mu$m) channel of Fig. 2 showing oscillations in transverse size.

about 200 μm from the original target position. Beyond that density, it self-focuses into the channel. At the time the interferogram was taken, the density channel formed by the short pulse had already expanded to a size of about 25 μm in diameter. Abel inversion of the density profile suggests that the density depression inside the channel was about 0.4 times the background density. In interferograms obtained at earlier times, the density depression could not be measured, since the phase variation was below the resolution of the interferometer.

The experiment has been simulated with the 3D PIC code VLPL (Virtual Laser Plasma Laboratory), recently developed for massive parallel processing (MPP). It extends the single-processor code LPlas3D [10] and was run on 32 processors of the CRAY-T3D at the Rechenzentrum Garching. The simulation results are presented in Figs. 5 and 6. The density profile and beam parameters of the experimental case of Fig. 2 were used. The code follows the dynamics of about 2×10^7 electrons and 7×10^6 ions on a $800 \times 100 \times 100$ spatial mesh. This corresponds to 3 electrons and 1 ion per cell. The longitudinal density gradient is modeled by using particles with different weights, but the same charge-to-mass ratio [15] such that, initially, each cell in the plasma region contains the same number of particles.

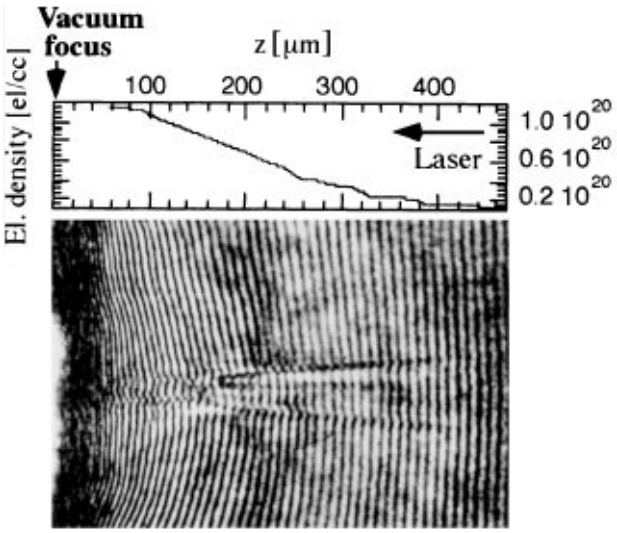

FIG. 4. Interferogram taken 5 ps after the interaction of the short pulse, at similar irradiance as in Fig. 2, with the preformed plasma (the density of the preformed plasma along the laser axis is also shown).

The simulation box is shown in Fig. 5(a). The laser pulse ($\lambda = 1.054\ \mu$m), polarized in the Z direction, is incident from the right with an incident irradiance of $I_0 = 8 \times 10^{18}$ W/cm^2 and a 12λ (FWHM) transverse Gaussian profile, giving a power of 10 TW. The intensity distribution $\langle I \rangle$ is shown in Fig. 5(a) for a time close to the peak of the pulse. After an initial unstable phase, the incident beam self-focuses into a narrow single channel at a density of about $0.07 n_c$. This process has been described in [10]. Here we show the first 3D-PIC results of channel formation for a laser propagating up a density gradient. The channel width pulsates as the pulse defocuses and refocuses with a characteristic period of $15-30\lambda$. The maximum intensity $\langle I_{\max} \rangle$ plotted in Fig. 5(b) varies accordingly with peaks up to $10 I_0$. These results closely reproduce the experimental observations. The channel of Fig. 5 is further analyzed in Fig. 6 by plotting the electron density for a Y-Z cross section at $X = 80\lambda$ and also as a line profile, normalized to the critical density n_c. One observes that electrons are expelled from the channel region and form a radially outgoing shock. The central density is about half of the ambient density with a peak on the axis due to magnetic pinching [10].

An important feature governing the channel dynamics are currents of relativistic electrons traveling with the light beam and generating quasistationary magnetic fields [10]. The simulation predicts 1–30 MeV electrons and magnetic fields rising from a few MG at the entrance up to 120 MG in the dense plasma region. In the snapshot of Fig. 5(a), the leading edge of the beam is seen to bend. Actually, this bending changes direction

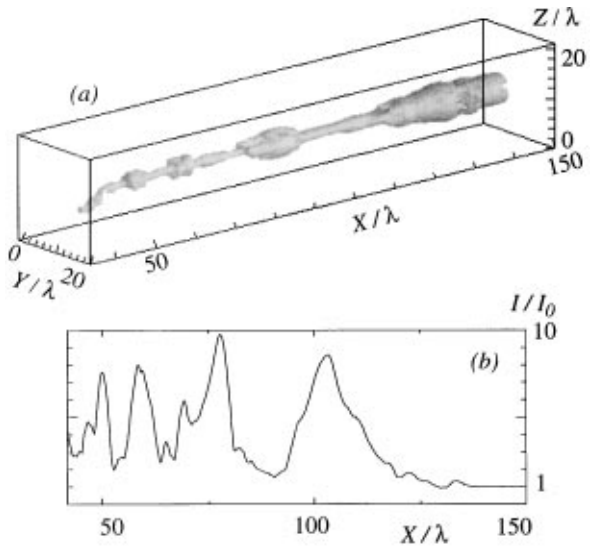

FIG. 5. Results of 3D PIC simulations based on the density profile of Fig. 2: (a) a perspective snapshot of the self-focusing pulse after 150 laser cycles (i.e., about 0.5 ps); the plotted surface corresponds to 67% of the cycle-averaged maximum intensity $\langle I_{\max} \rangle$. X is the distance from the original target position. (b) maximum intensity $\langle I_{\max} \rangle$ along the channel in units of the incident intensity I_0.

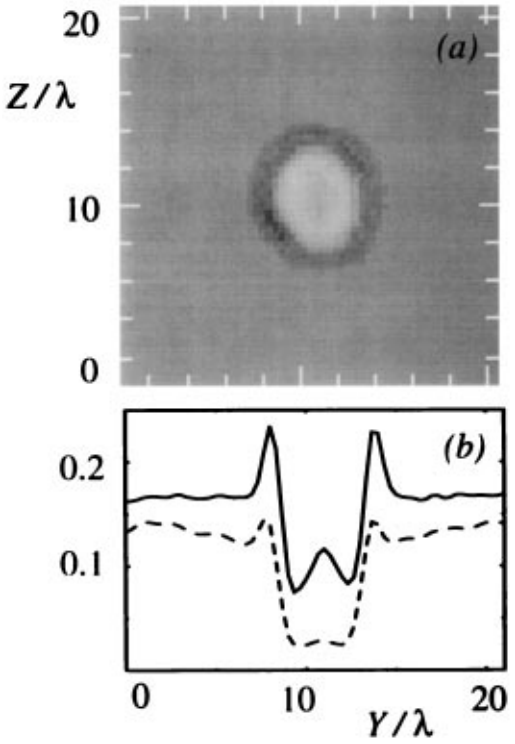

FIG. 6. Electron density in units of the critical density n_c for Y-Z plane at $X = 80\lambda$, after 150 laser cycles: (a) 2D plot using linear grey scale; (b) cut through center in Y direction: n_e/n_c (solid line), $n\langle\gamma^{-1}\rangle/n_c$ (dashed line).

in time and, as the front moves further to the left, the channel behind it straightens out. This is attributed to the stabilization effect of the fast electrons in the forward direction. These relativistic electrons modify the index of refraction n_r in the neighborhood of the channel. This can be seen in Fig. 6, where the quantity $n\langle\gamma^{-1}\rangle/n_c = 1 - n_r^2$ is plotted as a dashed line (the factor $\langle\gamma^{-1}\rangle$, locally averaged, accounts for the mass increase). A "relativistic valley" has formed, about 20 λ wide. At its center, a deeper density depression is produced by both electron expulsion and relativistic effects, and most of the light is guided into it.

Time-integrated spectra of the backscattered second harmonic radiation were also collected. The main feature observed was a redshifted broadening of the 2ω spectra, typically up to 40–50 nm. The broadening of the 2ω spectra can be explained as a self-phase-modulation (SPM) effect in the context of the channeling assumption discussed above [16]. During the channel formation, the pulse travels through a medium in which the refractive index is rapidly varying. As a consequence, its phase is modulated. Since the derivative of the refractive index stays positive during the pulse propagation, the broadening is on the red side of the spectrum. The order of magnitude of the broadening expected, $\Delta\lambda/\lambda$, can be estimated supposing that the pulse propagates, during the channel formation, in an initially uniform plasma, $\Delta\lambda/\lambda \approx L\Delta n_r/(c\tau)$, where L is the length of the channel, Δn_r the maximum variation of refractive index, c the speed of light, and τ the cavitation time. Using parameters close to the experimental ones, such as $L = 130$ μm, $\tau = 0.5$ ps, $\Delta n_r = 0.07$ [as in Fig. 6(b)], and $\lambda = 0.5$ μm, one obtains $\Delta\lambda \approx 30$ nm, which is of the same order of magnitude of the measured broadenings.

In conclusion, the formation of a single channel during the propagation of a picosecond pulse through preformed plasma has been observed far above threshold for relativistic filamentation, both experimentally and in computational simulations. The channeling was detected through optical probing measurements. Spectra of the second harmonic emission were also consistent with the channeling scenario. Simulations, performed with the 3D PIC code VLPL and based on experimental plasma conditions, closely reproduced the observed phenomena. The simulations revealed that relativistic electrons traveling with the light pulse and self-generated multimegagauss magnetic fields play a fundamental role in the channel formation.

The authors would like to acknowledge the help received by the staff of the Central Laser Facility while preparing and undertaking the experiment. This work was funded by an ESPRC/MoD grant. The simulation was supported in part by BMBF (Bonn) and EURATOM.

*Present address: IFAM-CNR, Pisa, Italy.
†On leave from Moscow Institute for Physics and Technology, Dolgoprudny, 141700, Russia.

[1] E. Esarey *et al.*, IEEE Trans. Plasma Sci. **24**, 252 (1996); D. Umstadter *et al.*, Science **273**, 472 (1996); A. Modena *et al.*, Nature (London) **377**, 606 (1995).
[2] M. Tabak *et al.*, Phys. Plasmas **1**, 1621 (1994).
[3] S. Rae, Opt. Commun. **97**, 25 (1993); A. J. Mackinnon *et al.*, Phys. Rev. Lett. **76**, 1473 (1996).
[4] G. C. Durfee III and H. M. Milchberg, Phys. Rev. Lett. **71**, 2409 (1993); A. J. Mackinnon *et al.*, Inst. Phys. Conf. Ser. **140**, 337 (1995).
[5] P. Sprangle and E. Esarey, Phys. Fluids B **4**, 2241 (1992); A. Chiron *et al.*, Phys. Plasmas **3**, 1373 (1996).
[6] A. B. Borisov *et al.*, Phys. Rev. Lett. **68**, 2309 (1992).
[7] A. B. Borisov *et al.*, J. Opt. Soc. Am B **11**, 1941 (1994); P. Monot *et al.*, Phys. Rev. Lett. **74**, 2953 (1995).
[8] P. E. Young *et al.*, Phys. Rev. Lett. **75**, 1082 (1995).
[9] P. E. Young and P. R. Bolton, Phys. Rev. Lett. **77**, 4556 (1996).
[10] A. Pukhov and J. Meyer ter Vehn, Phys. Rev. Lett. **76**, 3975 (1996).
[11] C. Danson *et al.*, in Proceedings of the 24th ECLIM, Madrid, 1996 (to be published).
[12] R. Benattar, C. Popovics, and R. Sigel, Rev. Sci. Instrum. **50**, 1583 (1979).
[13] J. P. Christiansen, D. E. F. T. Ashby, and K. V. Roberts, Comput. Phys. Commun. **7**, 271 (1974).
[14] J. A. Stamper *et al.*, Phys. Fluids **28**, 2563 (1985).
[15] J. Denavit, J. Comput. Phys. **9**, 75 (1972).
[16] D. Giulietti *et al.*, Opt. Commun. **106**, 52 (1994).